ELSEVIER

Contents lists available at ScienceDirect

Applied Catalysis A, General

journal homepage: www.elsevier.com/locate/apcata





Oxidative coupling of methane using oxidant mixtures of CO₂ and O₂ over Sr/La₂O₃

Hyewon Lee, William F. Northrop

Department of Mechanical Engineering, University of Minnesota, Minneapolis, MN 55455, USA

ARTICLE INFO

Keywords:
Oxidative coupling of methane
Carbon dioxide

ABSTRACT

Oxidative coupling of methane with CO_2 (CO_2 -OCM) is beneficial because it avoids complete oxidation, an undesired reaction that occurs during O_2 -oxidative coupling of methane. Previous literature has sparsely considered the respective roles of CO_2 and O_2 as reactants at CO_2 -OCM reaction conditions. This work explores the roles of CO_2 and O_2 in OCM over Sr/La_2O_3 with different reactant oxidant mixtures. While CO_2 alone did not significantly activate methane at 875 °C, a tenfold increase in C_2 yield resulted from adding 2 % O_2 . The role of CO_2 in heterogeneous reactions was supported by XPS and XRD, which showed presence of carbonate species on the catalyst surface while the bulk phase remained La_2O_3 . The work shows that a small amount of gaseous oxygen in the reactants can greatly improve methane conversion, and while oxygen is crucial in converting methane, CO_2 plays an important role during ethane dehydrogenation.

1. Introduction

Although the price of natural gas (NG) varies widely on the world market, global reserves remain high for the foreseeable future. NG has the lowest molecular carbon to hydrogen ratio of any fossil fuel, resulting in lower CO₂ emissions when consumed in industrial processes like syngas production or ammonia synthesis. A promising alternative to cracking liquid hydrocarbons for ethane and ethylene production is to use NG as a feedstock for catalytic oxidative coupling of methane (OCM). Since its discovery in the 1980's, OCM has been considered an important process for producing value-added chemicals like ethylene [1]. The most suitable catalysts for OCM are basic metal oxides [2,3]. Commonly used materials include Mg/O, La $_2$ O $_3$, and Mn/Na $_2$ WO $_4$ /SiO $_2$ based catalysts. In particular, La2O3 based catalysts have shown moderate methane conversion and C₂ selectivity even at lower temperature, and more so when doped with metals such as Ba and Sr [3,4]. Under such operating conditions with La2O3 based catalysts, C2 yield achieved ranged from as low as 5 % at 500 °C with Sr/La₂O₃ coated monolith catalyst and as high as 18 % using binary La₂O₃-CeO₂ nanofiber catalyst [5,6]. Many proposed mechanisms for OCM suggest that the global reaction begins with H-abstraction by an active oxygen species on the catalyst surface. Methyl radicals then combine in the gas phase to form ethane and then ethylene through dehydrogenation. However, non-selective pathways for the oxidization of methyl radicals and

hydrocarbons also exist, producing carbon oxides. The tradeoff relationship between methane conversion and C_2 selectivity, i.e. increasing methane conversion leading to decreased C_2 selectivity, is a barrier to achieving the 25–30 % C_2 yield required for OCM commercialization [7]. Some attribute this crucial tradeoff to the use of O_2 , a strong oxidant that causes secondary oxidation of produced C_2 hydrocarbons [8].

To mitigate secondary oxidation of C_2 hydrocarbons, the use of soft oxidants has been examined. Among soft oxidant candidates, CO_2 has gained attention for several reasons. Its mild nature prevents secondary oxidation of the C_2 hydrocarbon products. Further, with CO_2 as a reactant, the OCM reaction becomes endothermic, which eliminates large temperature fluctuations in larger catalyst beds. One key disadvantage is that, due to the inertness of CO_2 , CO_2 -OCM over known catalyst materials, high temperature and added heat from an external source are required.

OCM with CO_2 as oxidant, CO_2 -OCM, can be expressed by the chemical equations shown in reactions R1 and R2.

$$2CH_4 + 2CO_2 \rightarrow C_2H_4 + 2CO + 2H_2O$$
 (1)

$$2CH_4 + CO_2 \rightarrow C_2H_6 + CO + H_2O$$
 (2)

The changes in Gibbs free energy (ΔG°) at 298 K of R1 and R2 are 226.88 kJ/mol and 97.31 kJ/mol, respectively. Their corresponding enthalpy changes are (ΔH°) are 284.36 kJ/mol and 106.2 kJ/mol. This

^{*} Correspondence to: University of Minnesota, MN 55455, USA. *E-mail address*: wnorthro@umn.edu (W.F. Northrop).

indicates that the reaction is thermodynamically unfavorable at standard conditions and that the reactions are endothermic. However, many studies have proven that the reactions are viable at elevated temperatures. Nishiyama and Aika were one of the first to demonstrate that CO2 could be used as oxidant for OCM over PbO-MgO catalyst and that, through isotope experiments, the source of CO was CO₂, not CH₄ [9]. Asami et al. studied a series of metal oxides for CO2-OCM at 950 °C and concluded that rare earth catalysts show high C2 selectivity with yttrium resulting in the best C2 yield [10]. Xu et al. clarified the role of CO2 and suggested that the oxygen deficient sites on the catalyst surface were replenished by CO₂ to form O_(surface) which then abstracts H from CH₄ to form methyl radicals [11]. Xu et al. also observed that over 90 % of CH₄ was converted to C2 hydrocarbons which corroborates the findings of Nishiyama and Aika that the source of carbon in C₂ products is methane. Cai et al. used Mn-SrCO₃ to show that lattice oxygen does not play a role during CO₂-OCM and that oxygen from CO₂ is the active oxygen species that produces C2 hydrocarbons. The same trend was observed as reaction temperature was increased, achieving the highest C₂ yield of 5.1 % at 900 °C [12]. Early studies on CO₂-OCM demonstrated the potential of CO₂ as the oxidant for OCM and elucidated its role at high temperatures

Using CO2 for OCM has significant limitations in yield and conversion. Many catalysts have been explored to increase conversion efficiency and enable higher selectivity to C2 hydrocarbons during CO2-OCM. Wang et al. were able to achieve about 4 % C2 yield using CaO/ CrO₃, higher than C₂ yield achieved using pure CaO and Cr₂O₃ [13]. Mn-based binary oxide catalysts were found to be suitable, especially a Sr-Mn catalyst that exhibited the highest C2 yield at 6.3 % at 900 °C [14]. With nano-CeO₂/ZnO catalyst, which gave higher methane conversion than conventional catalyst formulations, maximum C2 yield was 4.79 % although carbon deposition was more severe [15]. Istadi et al. used CaO-MnO/CeO $_2$ catalysts to achieve 3.9 % C $_2$ yield while showing that both catalyst basicity and reducibility correlate with methane conversion and C2 yield for CO2-OCM [16]. One of the highest C2 yields of 6.6 % was reached with sodium and chloride added CaO-based catalyst at 950 °C [17]. While many catalysts have shown to be effective for CO₂-OCM, C₂ yield is low, ranging from 3-6 %. Conversely, O2-OCM typically has C2 yield close to 20 %.

The effect of small quantities of CO_2 on O_2 -OCM catalysis has been studied under operating conditions relevant for O_2 -OCM; methane-to-oxygen (C/O) ratios of 3–5 and operating temperatures from $600-800\,^{\circ}$ C. The effect has been studied over many catalysts, including La_2O_3 -based materials because CO_2 is the major carbon oxide byproduct of OCM and is known to affect performance in several ways. Some have shown a positive effect of CO_2 including stabilization and increased C_2 selectivity [18,19] while many have found that CO_2 has a negative effect, including decreased methane conversion, decreased C_2 selectivity, and inhibition of methane activation, largely attributed to the creation of surface carbonates [11,20–24]. Although many have studied the impact of CO_2 under C_2 -OCM reaction conditions, few previous researchers have investigated OCM with both CO_2 and CO_2 under conditions relevant to CO_2 -OCM, marked by CO_2 /CH4 ratios between 1.0 and 2.0 and high temperatures in the range of 850–950 °C.

In this work, OCM over a range of $\rm O_2$ and $\rm CO_2$ concentration in the reactants is studied to investigate their individual performance and yield insights into their roles when used together at temperatures commonly employed for the $\rm CO_2$ -OCM reaction. Experiments were conducted under typical $\rm CO_2$ -OCM temperature and $\rm CO_2$ /CH₄ ratios with the addition of oxygen in the feed over $\rm Sr/La_2O_3$ catalyst. The roles of $\rm O_2$ and $\rm CO_2$ in such conditions are elucidated using the performance of the catalyst in each condition. Additionally, characterization of the catalyst under different mixtures of $\rm O_2$ and $\rm CO_2$ were performed using XPS and XRD to characterize the catalyst and its surface.

2. Experimental methodology

2.1. Benchtop experiments

A quartz tube reactor (7 mm I.D.) was packed with 500 mg of 1 wt % Sr/La₂O₃ catalyst (BET: $4.9 \text{ m}^2/\text{g}$, $250-350 \mu\text{m}$), provided by Johnson Matthey (UK). The provided catalyst was synthesized using the incipient wetness impregnation method [25]. An electric tube furnace (Lindberg Blue M) set to 875 °C was used to heat the reactor under N₂ (99.9999 %) at 50 ml/min (6000 ml/hr/ g_{cat}). It should be noted that the measured temperature was stable at slightly higher than the setpoint temperature at around 885 \pm 3 °C. The reactant mixture containing CO₂ (99.999 %), CH₄ (99.0 %), O₂ (99.996 %), and N₂ (99.9999 %) were fed to the reactor once the temperature reached the desired setpoint. CH₄ concentration in the feed was always kept the same throughout the experiments and the flow rate of 10 ml/min was held constant for all conditions. The flow rates of CO2, O2, and N2 were adjusted using mass flow controllers according to the conditions shown in Table 1 while maintaining the total flow rate at 50 ml/min to maintain constant gas hourly space velocity. For example, at CO₂/CH₄/O₂ of 1/1/0.1, the flow rates of CO₂, CH₄, and O₂ were 10 ml/min, 10 ml/min, and 1 ml/min, respectively. The flow rate of N₂ was set to 29 ml/min to achieve 50 ml/min overall. A cold trap was placed downstream of the reactor to remove any moisture before the effluent gas entered micro-GC (Inficon Micro GC Fusion® Gas Analyzer) for sample analysis. The Micro-GC was equipped with two columns, a Molsieve column for H2, O2, N2, CH4, and CO and a Rt U-Bond column for CO2, C2H6, C2H4, and C2H2. Carbon species balance was evaluated using Eqs. (3)–(5), where \dot{x} denotes the molar flow rate of a species. %Carbon loss was ensured to be within 5 %.

$$C_{in} = \dot{x}_{CH_4} + \dot{x}_{CO_2} \tag{3}$$

$$C_{out} = \dot{x}_{CH_4} + \dot{x}_{CO_2} + 2 * (\dot{x}_{C_2H_4} + \dot{x}_{C_2H_6} + \dot{x}_{C_2H_2}) + \dot{x}_{CO}$$
(4)

$$% Carbon loss = \frac{(C_{in} - C_{out})}{C_{in}} \times 100$$
 (5)

The performance of the catalyst was evaluated by calculating methane conversion, CO_2 conversion, C_2 selectivity, and C_2 yield (Eqs. (1)–(4)). In these equations, \dot{x} denotes the molar flow rate of a species.

$$X_{CH_4} = \frac{(\dot{x}_{CH_4,in} - \dot{x}_{CH_4,out})}{\dot{x}_{CH_4,in}} \tag{6}$$

$$X_{CO_2} = \frac{(\dot{x}_{CO_2,in} - \dot{x}_{CO_2,out})}{\dot{x}_{CO_2,in}} \tag{7}$$

$$S_{c_2} = \frac{2 \bullet \left(\dot{x}_{C_2 H_6} + \dot{x}_{C_2 H_4} + \dot{x}_{C_2 H_2} \right)}{\dot{x}_{C H_4, in} \bullet X_{C H_4}}$$
(8)

$$Y_{C_2} = X_{CH_4} \bullet S_{c_2} \tag{9}$$

2.2. Catalyst characterization

To better understand the bulk structure and the surface under different mixtures of O_2 and CO_2 , catalyst samples were treated under three types of oxidant flows: A) $2\,\%\,O_2+20\,\%\,CO_2$, B) $2\,\%\,O_2$, and C) $20\,\%\,CO_2$ at 875 °C. To prepare the samples, the catalyst was placed in a 4 mm I.D. tube, and the temperature was ramped to 875 °C under N_2 flow. Once the setpoint temperature was reached, N_2 was replaced by the oxidant flow and then remained under the condition for 30 min. Then, the furnace was turned off and the temperature was decreased rapidly under N_2 .

X-ray diffraction (XRD) was used to determine the bulk structure of the catalyst and x-ray photoelectron spectroscopy (XPS) was used to identify the surface composition. XRD patterns were obtained using Bruker D8 Discover with Co K α radiation (40 kV, 35 mA, $\lambda = 1.789$ nm).

Table 1
Feed flow rates for the benchtop experiments and their corresponding CO₂/CH₄ and CH₄/O₂.

O ₂ -lean CO ₂ -OCM			O ₂ -rich CO ₂ -OCM			O ₂ -OCM	
CO ₂ /CH ₄ /O ₂ [ml/min]	CO ₂ /CH ₄ [dimensionless]	CH ₄ /O ₂ [dimensionless]	CO ₂ /CH ₄ /O ₂ [ml/min]	CO ₂ /CH ₄ [dimensionless]	CH ₄ /O ₂ [dimensionless]	CO ₂ /CH ₄ /O ₂ [ml/min]	CH ₄ /O ₂ [dimensionless]
5/10/1	0.5	10	5/10/3	0.5	3.33	0/1/0.1	10
10/10/1	1	10	10/10/3	1	3.33	0/1/0.3	3.33
15/10/1	1.5	10	15/10/3	1.5	3.33		
20/10/1	2	10					

XPS spectra were obtained using PHI 5000 VersaProbe III Photoelectron Spectrometer. For XPS analysis, to prevent surface contamination, the quartz tube was transferred to a glovebox with N_2 still in the reactor. In the glovebox, the samples were transferred to an air-free vessel for XPS analysis.

3. Results and discussion

3.1. CO₂-OCM over Sr/La₂O₃

The activity of Sr/ La₂O₃ catalyst for pure CO₂-OCM was first determined to provide a baseline for later experiments with added O₂. The highest C₂ yield achieved was 0.6 % at CO₂/CH₄ = 0.5 % and 0.2 % C₂ yield at CO₂/CH₄ = 2. The C₂ yields found were on a similar order of magnitude to that of the experiment conducted with La₂O₃ by Asami et al. [10]. They obtained approximately 0.23 % C₂ yield while operating at CO₂/CH₄ = 2 over 2 g of catalyst. Experimental results showed that methane conversion ranged between 1.9 % and 3.9 % depending on the CO₂/CH₄. Sr/La₂O₃ is not sufficiently active towards C₂ hydrocarbon formation during pure CO₂-OCM. Inactivity could be due to the formation of carbonate species on the catalyst surface or the lack of gaseous oxygen in the feed. It should be noted that CO₂ dissociation could have occurred as CO was the highest concentration species in the products.

3.2. O2-lean CO2-OCM

It has been established by this study and others that pure CO_2 -OCM over Sr/La_2O_3 yields less than 1 % C_2 hydrocarbons in the products; therefore, CO_2 alone cannot be used as oxidant at practical reactor

temperatures. To investigate whether oxygen in the reactants improves performance of CO₂-OCM, a small amount of oxygen, corresponding to 2 % oxygen in the feed, replaced N₂, maintaining the same total flow rate. Fig. 1 shows the performance of O₂-lean CO₂-OCM over CO₂/CH₄ ratios from 0.5 to 2 at 875 °C. Based on the amount of oxygen in the feed, a methane-to-oxygen (C/O ratio) of 10 was maintained through this set of experiments. A methane-to-oxygen (C/O) ratio of 10 is well above the ratio (3–6) that is typically used for O₂-OCM.

Fig. 1 shows that for all CO_2/CH_4 ratios, methane conversion ranged from 9.4 % to 10.5 % and C_2 selectivity ranged from 68 % to 73 %. Both results combined led to a C_2 yield of 6.7 - 7.9 %. Both $CO_2/CH_4 = 0.5$ and 1 cases resulted in almost the same methane conversion and C2 selectivity, and thus C2 yield. With added O2 methane conversion and C2 yield were found to be significantly higher when compared to the results reported in Section 3.1. The experimental condition with 2 % oxygen in the reactants resulted in a more than two-fold increase in both parameters. The C_2 selectivity of 68 - 73 % is also close to the target C_2 selectivity for OCM commercial viability [7,26,27]. The best performance was achieved at $CO_2/CH_4 = 1$, while decreasing performance was shown in terms of decreased methane conversion and C2 selectivity at CO₂/CH₄ higher than 1. Decreasing methane conversion with increasing CO2 concentration was also observed over Na2WO4/Mn/SiO2 catalyst and was attributed to the structural change of the catalyst in which active species decreased and inactive species increased [28]. A similar reason can describe the decreasing performance parameters with increasing CO₂. Chu et al. proposed that a La³⁺- O²⁻ cluster in the La₂O₃ material transforms into La^{3+} - CO_3^{2-} when La_2O_3 reacts with CO_2 . The new cluster is less basic than La³⁺- O²⁻ clusters, inhibiting the methane activation reaction on the surface [29]. The creation of active

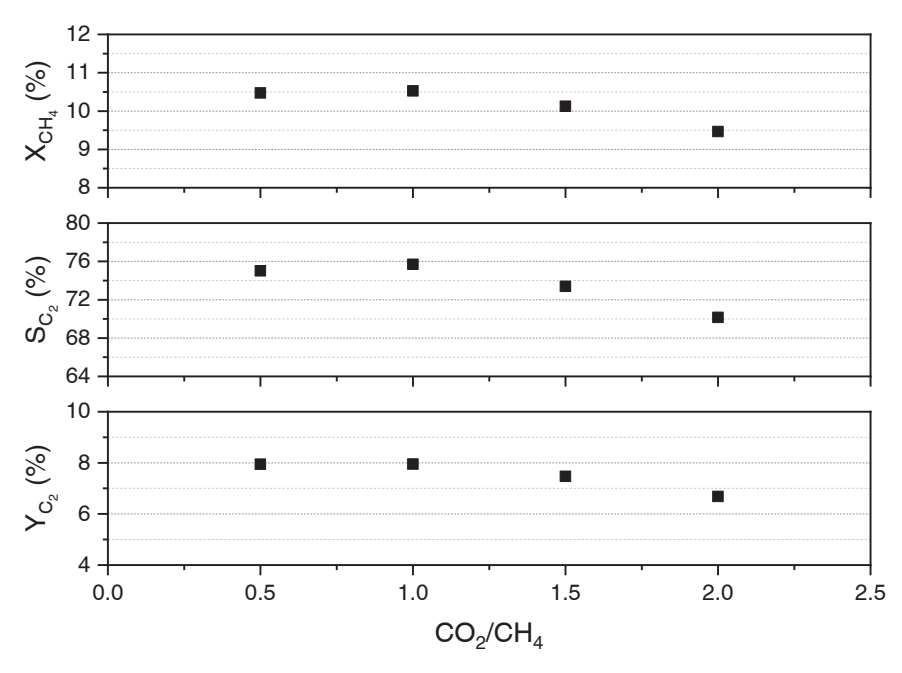
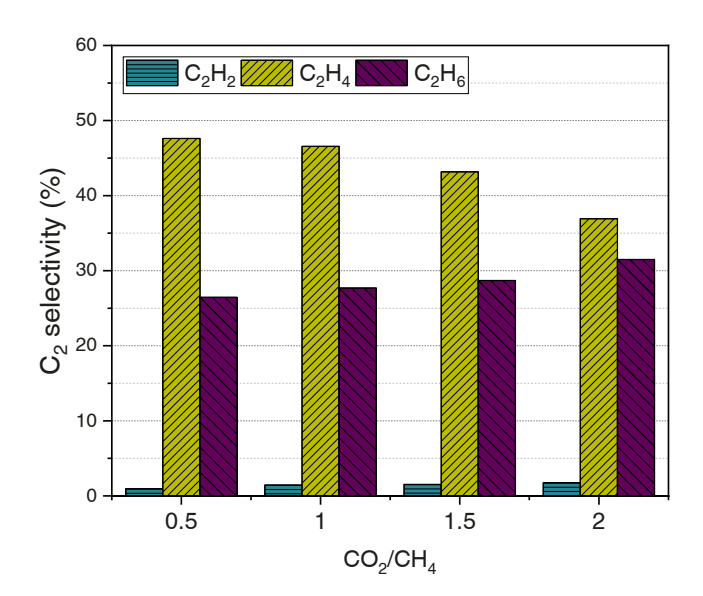


Fig. 1. Methane conversion, C2 selectivity, and C2 yield for CO2-OCM with 2 % oxygen over CO2/CH4 = 0.5-2 at 875 °C using 500 mg Sr/La2O3.

site-blocking carbonate species has been discussed many times in literature [24,29]. The experiments completed here indicate that gaseous oxygen in the feed is critical for converting methane into methyl radicals and achieving significant methane conversion $\rm Sr/La_2O_3$ catalysts. Also, when $\rm CO_2$ exceeds certain amount, i.e. at $\rm CO_2/CH_4$ ratio higher than 1, the poisonous effect of $\rm CO_2$ is evident.

Fig. 2 shows selectivity for C_2 hydrocarbons and ethylene-to-ethane ratio plotted over the CO_2/CH_4 range to illustrate the effect of increasing CO_2 on each C_2 hydrocarbon. Ethane is the first C_2 hydrocarbon product to be formed in OCM, which then is converted to ethylene via dehydrogenation and then to acetylene. In the experiments, acetylene selectivity remained low, while ethylene selectivity decreased with increasing CO_2/CH_4 ratio. Ethane selectivity continued to increase with increasing CO_2/CH_4 . In all cases, selectivity towards ethylene remained higher than the selectivity to ethane. With increasing amount of CO_2 at a fixed amount of CO_2 , the increase in ethane and decrease in ethylene suggest that CO_2 prevents dehydrogenation of ethane to ethylene when present in excess, as shown in cases $CO_2/CH_4 = 1.5$ and 2. Many mechanisms propose that dehydrogenation of ethane occurs via surface reaction [30,31] while others suggest that it occurs through a gas phase reaction mechanism [32]. Regardless, Fig. 2 serves as the evidence that



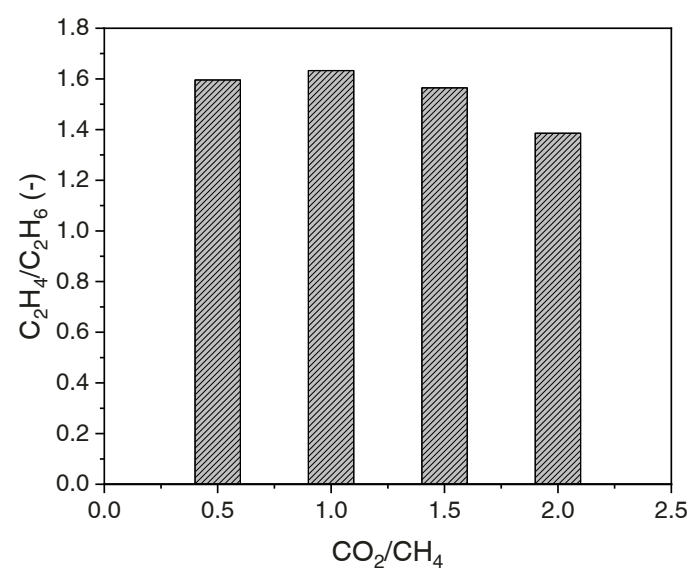


Fig. 2. Selectivity of C_2 hydrocarbons (top) and ethylene-to-ethane ratio (bottom) at $CO_2/CH_4=0.5-2$ at 875 °C during O_2 -lean CO_2 -OCM.

excess CO₂ prevents ethane dehydrogenation to ethylene.

3.3. O₂-lean CO₂-OCM comparison to O₂-OCM and non-catalytic O₂-OCM

The results discussed so far show that the presence of oxygen in the feed is crucial in producing ethylene via oxidative coupling of methane with CO₂ over Sr/La₂O₃. However, at high temperatures like 875 °C, it is of interest to demonstrate that the production of C₂ hydrocarbons is from heterogeneous reactions and not homogeneous reactions in the gas phase. Thus, the results from O₂-lean CO₂- OCM were compared to those of non-catalytic O₂-OCM and O₂-OCM. Non-catalytic O₂-OCM at C/O=10 was performed in a blank quartz tube and its result are only included to show the activity of Sr/La₂O₃ at high temperature. It is noted that the typical temperature range of O₂-OCM of 600 °C - 800 °C and C/O ratio of 3–5; the conditions given here are not ideal for O₂-OCM. Based on the results from Fig. 2, CO₂/CH₄ = 1 ratio was chosen for comparison as it had the highest C₂ yield. The operating conditions for subsequent experiments are listed in Table 2.

As shown in Fig. 3, non-catalytic OCM in the gas phase led to 5 % methane conversion and 32 % C2 selectivity, which indicates that the dominant reaction was the complete/partial oxidation of hydrocarbons. Also, oxygen conversion was only 20 % without a catalyst, which is much lower than 100 % oxygen conversion observed during catalytic O2-OCM and O2-lean CO2-OCM. Methane conversion during catalytic O₂-OCM was the highest at 13.1 %, while C₂ selectivity was close to 60 %, resulting in a C2 yield of 7.5 %. This adds further evidence that the catalyst retained its activity at 875 °C, though Sr/La₂O₃ is known to be an active catalyst at a lower temperature range. For comparison, Choudhary et al. looked at various La₂O₃ containing catalyst at 850 °C and C/O= 16 and reported C2 yields of 1.6-10.1 % [33]. Although performance differs depending on many parameters, ethylene-to-ethane ratio and methane conversion are expected to be high at high temperature which is what was observed in this study. In particular, the ethylene-to-ethane ratios says that more ethane is present when CO₂ is present in the feed. Fig. 4 further clarifies what was observed in terms of C2 hydrocarbons.

Fig. 4 shows that both ethane and ethylene selectivity greatly improved during O₂-lean CO₂-OCM. The main contribution to improved selectivity of O2-lean CO2-OCM came from the increased in ethane selectivity, which more than doubled during CO2-OCM. A few possibilities can describe the increased C2 selectivity. One possibility is the creation of active oxygen species from CO2 dissociation reaction. As mentioned previously, CO2 dissociates into CO and a surface oxygen species on the catalyst surface. The results showed that CO selectivity is much higher when CO₂ is present in the feed in all cases. With CO₂ concentration in the feed, the concentration of the surface species would be created in addition to the ones from O₂ adsorption. It is unlikely that the surface oxygen species from CO₂ contributes to methane activation to create methyl radicals as seen in Fig. 3. However, it is possible that the surface oxygen species played a role in abstracting hydrogen from ethane to create ethylene in a process called CO2-assisted oxidative dehydrogenation of ethane (CO2-ODH) [34]. The role of CO2 in this reaction would be in site regeneration through dissociation into CO and surface bound oxygen. CO2-ODH of propane to propylene was investigated over MoO₃/La₂O₃-γAl₂O₃ in which increase in La₂O₃ content correlated with decreasing activity but increasing alkene selectivity

Table 2 Feed compositions for non-catalytic O_2 -OCM, O_2 -OCM and O_2 -lean CO_2 -OCM.

	CO ₂ /CH ₄ /O ₂ [ml/min]	CH ₄ /O ₂ [dimensionless]	CO ₂ /CH ₄ [dimensionless]
Non-catalytic O ₂ -OCM	0/10/1	10	-
O ₂ -OCM	0/10/1	10	-
O ₂ -lean CO ₂ -OCM	10/10/1	10	1

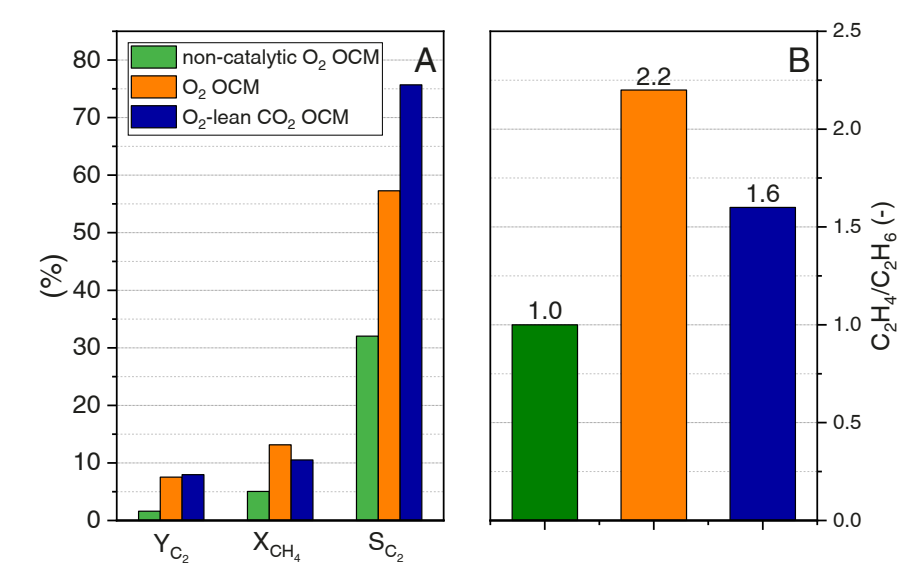


Fig. 3. Comparison of C_2 yield, methane conversion, and C_2 selectivity (left) and ethylene-to-ethane ratio (right) in non-catalytic O_2 -OCM (green), O_2 -OCM (orange) and O_2 -lean CO_2 -OCM (blue) at CO_2 -CCH = 1 at 875 °C.

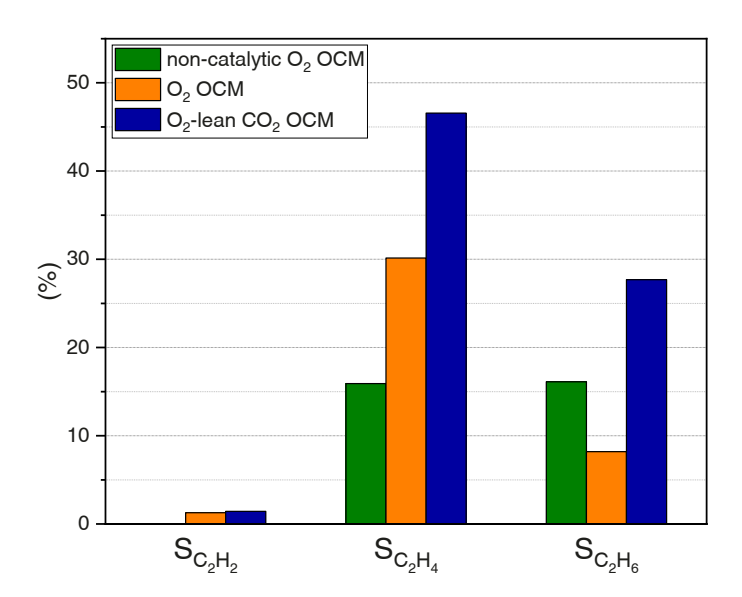


Fig. 4. Comparison individual C2 hydrocarbon selectivity for non-catalytic O2-OCM (green), O2-OCM (orange) and O2-lean CO2- OCM (blue).

[35]. This finding is similar to what is observed here, where CO_2 led to decrease in methane activation and increase in ethylene selectivity. Simultaneously, CO produced during $\mathrm{CO}_2\text{-}\mathrm{OCM}$ can suppresses CO production from CH_4 . CO produced from $\mathrm{O}_2\text{-}\mathrm{OCM}$ results from the oxidation of hydrocarbons. CO during $\mathrm{CO}_2\text{-}\mathrm{OCM}$ is produced mainly from CO_2 dissociation into CO and O. The desorbed CO in the atmosphere would then drive the equilibrium of CO production reaction to suppress CO production from methane, thus increasing C_2 selectivity.

Another possibility is that CO₂ efficiently prevents oxidation of the methyl radicals. Several OCM mechanisms propose that the pathway to carbon oxides begins by oxidation of methyl radicals both in the gas phase and on the surface. Martin and Mirodatos proposed a CO₂ formation mechanism in which methyl radical is oxidized by surface oxygen species consecutively to surface carbonates [36]. In CO₂-OCM, cases in which the abundance of CO₂ already forms carbonates, less sites are left for methyl oxidation, thus suppressing surface methyl oxidation. This can explain increased ethane selectivity. Yoon et al. reported oxygen from O₂ adsorption was responsible for methane activation and lattice oxygen was required not only for ethane dehydrogenation but

also for methyl oxidation to carbon oxides over $Na_2WO_4/Mn/SiO_2$ [37]. CO_2 present during O_2 -lean CO_2 -OCM, through carbonate production could have occupied active sites and left selective sites for dehydrogenation reactions. The same reasoning can be applied to the role of CO_2 in preventing oxidation of the hydrocarbons. Judging from the ethylene-to-ethane ratios in Fig. 3, it is probable that ODH of ethane more prevalent in O_2 -OCM than in CO_2 -OCM which had less available oxygen species.

To summarize the two possible scenarios that can be deduced from the reactor experiments, the common roles of CO_2 are: 1) suppressing the production of carbon monoxides while facilitating CO_2 -assisted oxidative dehydrogenation; and 2) suppressing oxidative dehydrogenation of ethane, which leads to the production of carbon oxides that decrease C_2 selectivity. In other words, the role of O_2 lies in oxidizing methane while CO_2 is responsible for oxidizing ethane.

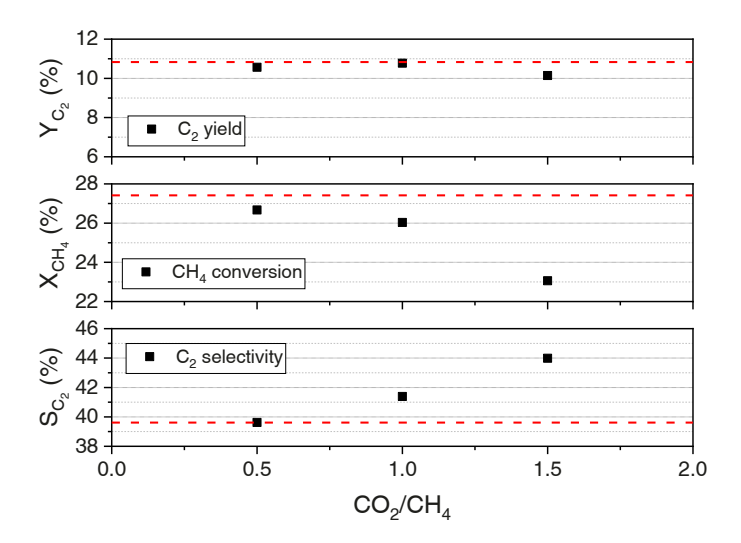
3.4. O₂-rich CO₂-OCM

To determine whether the increase in C2 selectivity and methane

conversion is observed under oxygen-rich condition, the oxygen concentration was increased to 6 % while keeping the methane and $\rm CO_2$ concentrations the same as the $\rm O_2$ -lean $\rm CO_2$ -OCM condition. The C/O ratio in this case was 3.33, which is typical for $\rm O_2$ -OCM. Fig. 5 shows the catalyst activity when the oxygen content in the feed is increased from 2 % to 6 % over $\rm CO_2$ concentration range from 10 % to 30 %.

Both O_2 -lean and O_2 -rich conditions showed similar trends in methane conversion and C_2 selectivity with increasing CO_2 , although it is more apparent during O_2 -rich conditions. Methane conversion increased by more than twofold from approximately 10 % to near 25 %. However, due to the decrease in C_2 selectivity, C_2 yield was only marginally higher than C_2 yield obtained during O_2 -lean conditions. Ethylene-to-ethane ratios shown in Fig. 5 ranges from 3–3.4, which is higher than the range obtained during O_2 -lean CO_2 -OCM of 1.2–1.4. This could be due to oxidative dehydrogenation of ethane facilitated by the higher oxygen concentration.

Fig. 6 shows CO_2 conversion achieved during O_2 -lean and O_2 -rich conditions are shown over CO_2/CH_4 range of 0.5–1.5. Positive CO_2 conversion indicates reduction of CO_2 while negative CO_2 conversion indicates production of CO_2 . With more oxygen available in the feed, there was a net increase in CO_2 despite its abundance in the feed to the



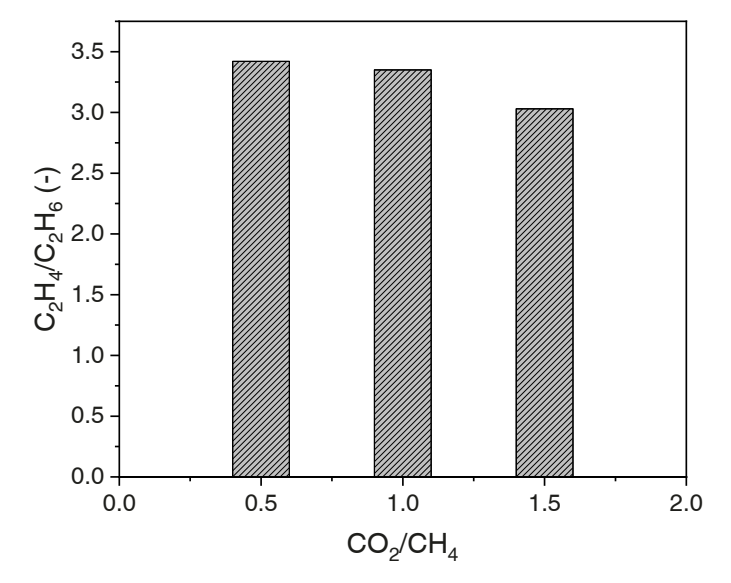


Fig. 5. Performance parameters during O_2 -rich OCM (top) and ethylene-to-ethane ratios (bottom). Red lines indicate conversion, selectivity, and yield during O_2 -OCM.

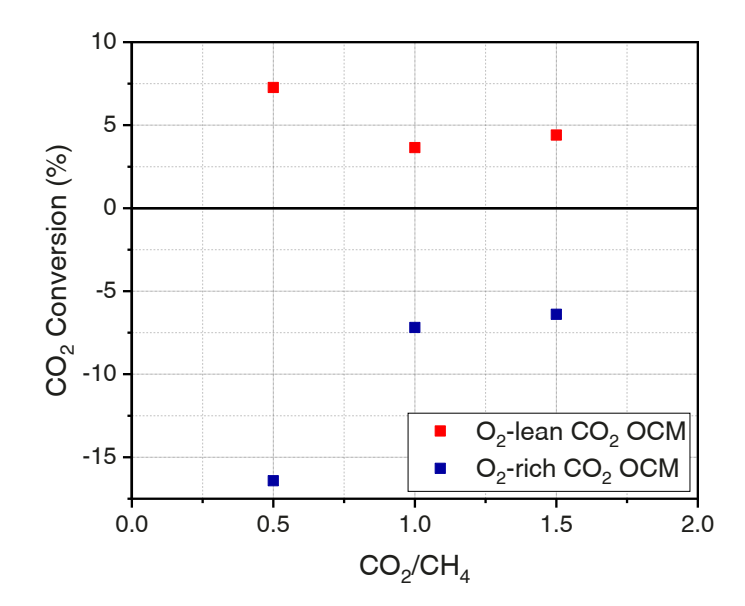


Fig. 6. CO₂ conversion of O₂-lean and O₂-rich CO₂-OCM.

reactor.

There are many sources of CO₂ during OCM when oxygen is present. Methyl radicals, as mentioned previously, can be oxidized in both gas phase and surface phase. The products of OCM, both ethane and ethylene, can be oxidized through secondary oxidation [38,39]. The decrease in C2 selectivity found from O2-lean CO2-OCM to O2-rich CO₂-OCM with increasing oxygen indicates that C₂ hydrocarbons were completely oxidized to carbon oxides. Also, ethylene-to-ethane ratio increased from 1.63 to 3.46. These indicate that ethane dehydrogenation reaction occurred more readily during O2-rich CO2-OCM, proceeding until they were fully oxidized. Parishan et al. proposed that the ethane undergoes gas phase thermal dehydrogenation reaction with gaseous oxygen to ethylene up until 800 °C [39]. Thermal dehydrogenation proceeds by $C_2H_6 \rightarrow C_2H_4 + H_2$. Because both O_2 -lean CO_2 -OCM and O₂-rich CO₂-OCM were at 875 °C, the only difference was the oxygen concentration and that was what resulted in higher ethylene amount. From this, it is implied that at high temperature, oxidative dehydrogenation is the major contributor in converting ethane to ethylene. With sufficient oxygen addition in the O2-rich condition, the reaction becomes closer to O2-OCM, in which oxidation of C2 hydrocarbons becomes a disadvantage that lowers C2 selectivity. While O₂-lean conditions is successful in utilizing CO₂ and increasing C₂ yield, O2-rich condition shows net increase in CO2.

3.5. XRD and XPS characterization

From Section 3.3 it was determined that in non-catalytic conditions, the reactions do not occur significantly in the gas phase. Also, while the role of CO_2 is important, it is not clear whether its role is in the gas phase or on the surface. Since O_2 is more reactive than CO_2 , it can be assumed that the role of CO_2 in the gas phase reaction would be less significant than what was obtained during non-catalytic O_2 -OCM. This means that the different performance in Fig. 3 is mostly due to the change in the structure of the catalyst in the bulk structure or its surface. To determine how the catalyst bulk structure and the surface changes under different mixtures of oxidants the three different samples are prepared. As stated in Section 2.2, the samples are treated under A) 2 % O_2 + 20 % CO_2 , B) 2 % O_2 , and C) 20 % CO_2 at 875 °C.

XRD on the three samples was first performed to determine the lattice structure of the catalyst to determine the role of CO_2 on the surface. All three XRD patterns can be matched to hexagonal La_2O_3 (PDF 00-002-0688) as shown in Fig. 5. It essentially shows that the bulk structure of

the catalyst remains the same under A) $2\% O_2 + 20\% CO_2$, B) $2\% O_2$, and C) $20\% CO_2$ flows, despite the large quantity of CO_2 in A and C. Fig. 7 also shows that (101) is the highest intensity peak in all cases, which shows that (101) is the preferred orientation regardless of the reactant.

The results from the XRD characterization are consistent with results from the literature that describe how La₂O₂CO₃ disintegrates into CO₂ and La₂O₃ at high temperature between 500–800 °C [21,40,41]. Fig. 8 shows the thermodynamic equilibrium mole percentage of CO₂ (X_{CO2}) at one atmosphere pressure over a temperature range from 600 °C to 900 °C for the reaction La₂O₃ + CO₂ \leftrightarrow La₂O₂CO₃. Since equilibrium X_{CO2} at 1 atm is 62.2 %, it is safe to say that, in all experiments performed here, the bulk structure of the catalyst remained La₂O₃.

Although CO₂ did not change the lattice structure of the catalyst in at the conditions studied in this work, using oxidant mixtures of CO₂ and O₂ led to different catalyst performance as shown in Figs. 2–4. Also, from the findings discussed in Section 3.3, the role of CO₂ appears to be crucial during heterogeneous OCM over Sr/ La₂O₃. XPS spectra of the three samples were performed to investigate the effect of different oxidants on the catalyst surface.

Fig. 9 shows the C1s and O1s spectra of Sr/La₂O₃ samples treated with: A) CO_2 ; B) O_2 ; and C) $CO_2 + O_2$. The adventitious peak at 285 eV was used as the internal standard. Two distinct peaks are 285 eV and 289.9 eV are found in all three spectra. The first peak at 285 eV is the adventitious C-C peak. The most apparent difference between the three C1s spectra is the presence of carbonate C peak at 289.9 eV in Fig. 9A and B due to the presence of CO₂ in the feed. A small carbonate peak was also observed in Fig. 9. B, though it is mostly likely due to contamination during sample transfer. While bulk structure remained La₂O₃ as shown Fig. 7, the surface of the catalyst is evidently affected by different concentrations of O2 and CO2. The area percentage of the carbonate peak is the highest in Fig. 9A, at 42.5 % followed by Fig. 9B at 35.5 % and then in Fig. 9C it decreased to 14.1 % in Fig. 9B. Comparable CO2 coverage in A and C, together with drastically different methane conversion in CO2-OCM and O2-lean CO2-OCM, show that the presence of CO2 and carbonate formation on the surface is the not sole reason for low methane conversion. The second peak at 290 eV is asymmetric for B and C, where oxygen is present. In both samples, an additional peak at 288.7 eV was required for deconvolution. This peak is often attributed to carboxyl group and/or incompletely oxidized carbon [42,43].

Fig. 10 shows O1s spectra of the three samples. All three show two distinct peak at 528.7 eV and 531.6 eV. The peak at 528.7 eV is the lattice oxygen of La₂O₃ peak [42,44,45]. The peak at 531.6 eV ranges

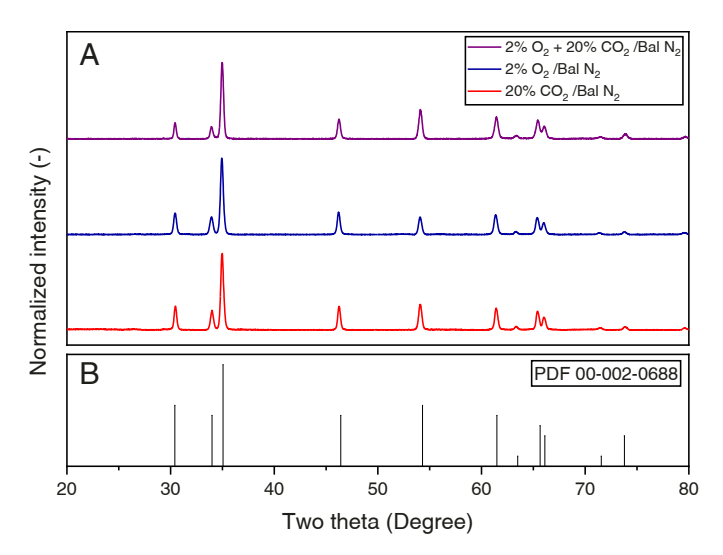


Fig. 7. (A) XRD patterns of La₂O₃ that underwent 1) 2 % O₂ + 20 % CO₂ 2) 2 % O₂, and 3) 20 % CO₂ at 875 °C and (B) XRD pattern reference PDF00–002-0688. Highest peak represents (101) plane.

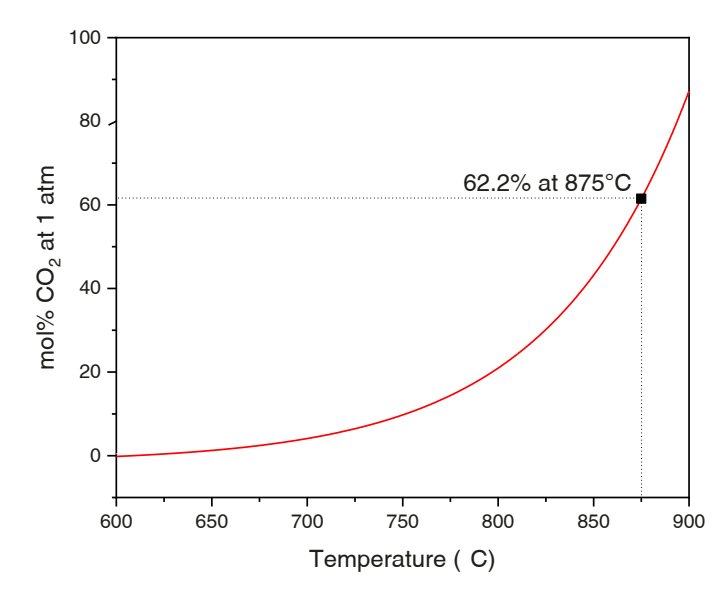


Fig. 8. Percentage of CO_2 at equilibrium for the formation of $La_2O_2CO_3$ at 1 atm. Calculated using the equation from [41].

from about 530 eV to 534 eV and is possibly a combination of several small peaks. From Fig. 9, it is known that carbonates are present on the surface in varying degrees. The calculated atomic ratio of $O_{531.6\,eV}$: C_{285 eV.carbonate} for A, B, and C were 3.9, 9.1, and 4.5. The atomic ratio of Ocarbonate: Ccarbonate is 3. The ratio for A is the closest to 3, which means that the peak at 531.6 eV in A consists mostly of carbonate peak, and minor peaks of other oxygen containing species. Similar conclusion can be drawn for C as well. For B, the ratio greatly exceeds 3, which shows that most of the oxygen-containing species on the catalyst surface are the ones other than lattice oxygen from La2O3 and carbonates. Possible candidates for oxygen-containing species whose position fall in the range of 530 eV and 534 eV are adsorbed water, hydroxyl groups, di-oxygen species, and partially oxidized carbon species found in C1s spectra [44-46]. Partially oxidized carbon species are minor contribution as can be seen in Fig. 9. Some degree of hydroxyl groups are expected as it easily forms on the surface of La₂O₃ [42]. Zhou et al. also proposed that peak correlated with catalytic activity was found at 531.5 eV [47]. Regardless, the carbonate coverage is the highest in A, followed by C and then B. In the two samples B and C that were treated with oxygen containing gas mixture, the sample with higher carbonate coverage had higher C_2 selectivity. This corroborates the conclusion drawn in Section 3.3 in which the role of CO2 was proposed to be in suppression of oxidative dehydrogenation of ethane to increase C2 selectivity. The order of lattice oxygen area is the reverse; B is the highest at 58.6 %, followed by C at 53.1 % and then A at 48.3 %. Considering the O $_{\rm 531.6~eV}\mbox{:}C_{\rm 285~eV,carbonate}$ of A and C and the relative area of the lattice oxygen coverage, the areas of carbonate coverage on the two samples is not drastically different. Additionally, Wang et al. proposed that lattice oxygen is responsible for methane activation and Palmer et al. proposed the formation of active site via the reaction between lattice oxygen and gaseous oxygen [48,49]. Although the identity of oxygen species for methane activation is still contentious, the experimental results and the XPS results both show that carbonate formation has less to do with methane activation and that gaseous oxygen, and consequently its adsorption on the surface, is crucial in achieving high methane conversion under operating conditions relevant to CO_2 -OCM.

4. Conclusion

In this study, oxidative coupling of methane (OCM) over Sr/La_2O_3 was performed across a range of CO_2/CH_4 ratios with added oxygen at

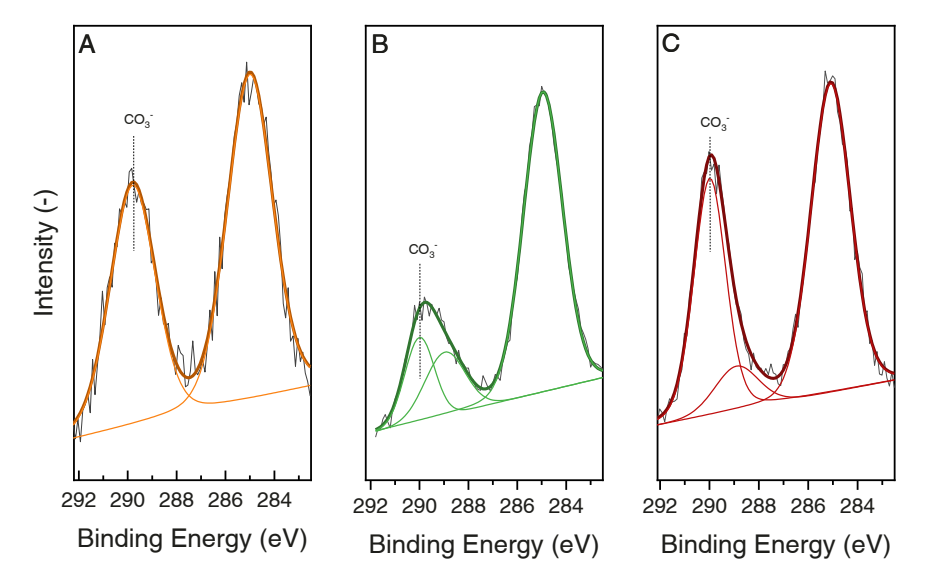
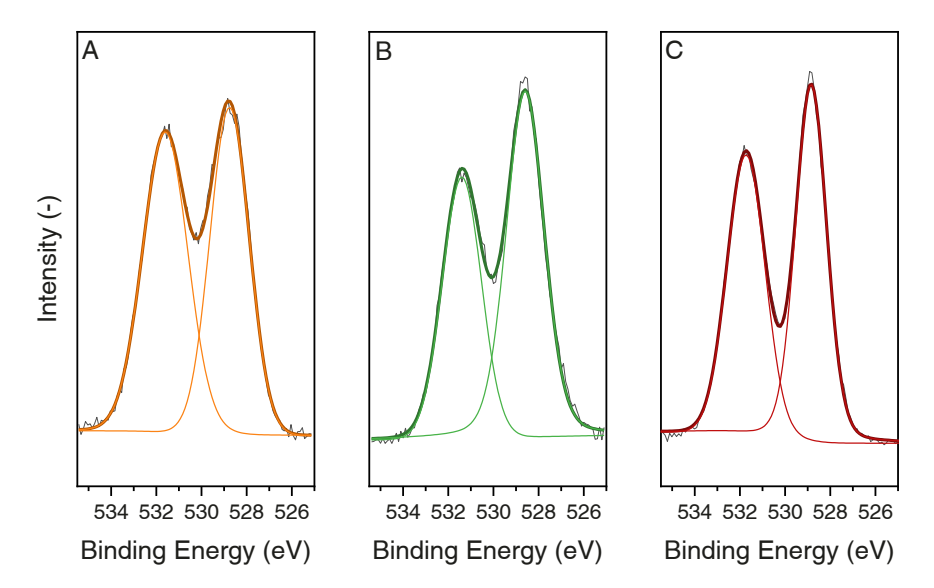


Fig. 9. C1s spectra of Sr/La_2O_3 treated at 875 °C under three different flows A) 20 % CO_2 , B) 2 % O_2 , and C) 20 % $CO_2 + 2$ % O_2 . Balance O_2 for all three conditions.



 $\textbf{Fig. 10.} \hspace{0.2cm} \textbf{O1s spectra of Sr/La}_2\textbf{O}_3 \hspace{0.2cm} \textbf{treated at 875 °C under three different flows A) 20 \% CO}_2, \hspace{0.2cm} \textbf{B) 2 \% O}_2, \hspace{0.2cm} \textbf{and C) 20 \% CO}_2 + 2 \hspace{0.2cm} \%\textbf{O}_2. \hspace{0.2cm} \textbf{Balance N}_2 \hspace{0.2cm} \textbf{for all three conditions.} \\ \textbf{O1s spectra of Sr/La}_2\textbf{O}_3 \hspace{0.2cm} \textbf{treated at 875 °C under three different flows A) 20 \% CO}_2, \hspace{0.2cm} \textbf{B) 2 \% O}_2, \hspace{0.2cm} \textbf{BO}_2, \hspace{0.2cm} \textbf{A) 20 \% CO}_2 + 2 \hspace{0.2cm} \texttt{MO}_2. \hspace{0.2cm} \textbf{Balance N}_2 \hspace{0.2cm} \textbf{for all three conditions.} \\ \textbf{A) 20 \% CO}_3, \hspace{0.2cm} \textbf{B) 2 \% CO}_3, \hspace{0.2cm} \textbf{A) 20 \% CO}_3,$

O₂-lean and O₂-rich conditions. While insignificant (0.2–0.5 %) C₂ yields were achieved during pure CO2-OCM, increased C2 yield of 6.7-7.9 % was possible with the addition of small amount of oxygen during O2-lean CO₂-OCM at 875 °C. Even at the high temperatures generally required for CO₂-OCM, CO₂ was not sufficient to activate methane over Sr/La₂O₃. For O₂-lean CO₂-OCM, 7.9 % was the highest C₂ yield achieved at CO₂/ $CH_4 = 1$. The measured selectivity of ethane and ethylene indicates that the role of CO₂ may lie in suppressing oxidative dehydrogenation (ODH) of ethane while facilitating CO2-assisted ODH. XRD was used to characterize the state of catalyst under high concentration of CO2 in the reactor and showed that the bulk structure of the catalyst remained hexagonal La2O3 regardless of the oxidant species. However, characterization of the catalyst surface with XPS proved that the catalyst surface changes significantly under different oxidant mixtures. CO2 is adsorbed to possibly participate in surface reactions of CO2-assisted oxidative dehydrogenation and suppresses oxidative dehydrogenation of ethane. The initial steps of H-abstraction from methane for methyl radical production is largely managed by oxygen, and the subsequent steps are influenced by CO₂ concentration that decides overall C₂ selectivity. In conclusion, this research shows that a small addition of oxygen to CO2-OCM greatly improves methane conversion and

consequently C_2 yield while taking the advantage of CO_2 in achieving high C_2 selectivity.

CRediT authorship contribution statement

William Northrop: Writing – review & editing, Supervision, Funding acquisition, Conceptualization. **Hyewon Lee:** Writing – review & editing, Writing – original draft, Visualization, Validation, Methodology, Investigation, Formal analysis, Conceptualization.

Declaration of Competing Interest

The authors have no competing interests to declare.

Data availability

Data will be made available on request.

Acknowledgements

This material is based upon work supported by the U.S. Department

of Energy's Office of Energy Efficiency and Renewable Energy (EERE) under Award Number DE-EE0008333. Parts of this work were carried out in the Characterization Facility, University of Minnesota, which receives partial support from the NSF through the MRSEC (Award Number DMR-2011401) and the NNCI (Award Number ECCS-2025124) programs. The authors would also like to acknowledge Nicolas Grosjean and Ben Rollins from Johnson Matthey for providing the catalyst material used in this work.

References

- [1] G. Keller, Synthesis of ethylene via oxidative coupling of methane I. Determination of active catalysts, J. Catal. 73 (1) (1982) 9–19, https://doi.org/10.1016/0021-9517(82)90075-6
- [2] F. Papa, P. Luminita, P. Osiceanu, R. Birjega, M. Akane, I. Balint, Acid-base properties of the active sites responsible for C2+ and CO₂ formation over MO-Sm2O3 (M=Zn, Mg, Ca and Sr) mixed oxides in OCM reaction, J. Mol. Catal. A: Chem. 346 (1–2) (2011) 46–54, https://doi.org/10.1016/j.moleata.2011.06.008
- [3] V.R. Choudhary, B.S. Uphade, S.A.R. Mulla, Oxidative coupling of methane over a Sr-promoted La₂O₃ catalyst supported on a low surface area porous catalyst carrier, Ind. Eng. Chem. Res. 36 (9) (1997) 3594–3601, https://doi.org/10.1021/ ie960676w.
- [4] J. Liu, et al., From fundamentals to chemical engineering on oxidative coupling of methane for ethylene production: a review, Carbon Resour. Convers. 5 (1) (2022) 1–14, https://doi.org/10.1016/j.crcon.2021.11.001.
- [5] B.M. Sollier, L.E. Gómez, A.V. Boix, E.E. Miró, Oxidative coupling of methane on Sr/La2O3 catalysts: Improving the catalytic performance using cordierite monoliths and ceramic foams as structured substrates, Appl. Catal. A: Gen. 532 (2017) 65–76, https://doi.org/10.1016/j.apcata.2016.12.018.
- [6] D. Noon, A. Seubsai, S. Senkan, Oxidative coupling of methane by nanofiber catalysts, ChemCatChem 5 (1) (2013) 146–149, https://doi.org/10.1002/ octs.201200408
- [7] E.V. Kondratenko, et al., Methane conversion into different hydrocarbons or oxygenates: current status and future perspectives in catalyst development and reactor operation, Catal. Sci. Technol. 7 (2) (2017) 366–381, https://doi.org/ 10.1039/C6CY01879C.
- [8] A.M. Arinaga, M.C. Ziegelski, T.J. Marks, Alternative oxidants for the catalytic oxidative coupling of methane, Angew. Chem. Int. Ed. 60 (19) (2021) 10502–10515, https://doi.org/10.1002/anie.202012862.
- [9] T. Nishiyama, K.-I. Aika, Mechanism of the oxidative coupling of methane using C02 as an oxidant over PbO?MgO, J. Catal. 122 (2) (1990) 346–351, https://doi org/10.1016/0021-9517(90)90288-U.
- [10] K. Asami, T. Fujita, K. Kusakabe, Y. Nishiyama, Y. Ohtsuka, Conversion of methane with carbon dioxide into C2 hydrocarbons over metal oxides, Appl. Catal. A: Gen. 126 (2) (1995) 245–255, https://doi.org/10.1016/0926-860X(95)00042-9.
- [11] X. Yide, Y. Lin, and G. Xiexian, Effect of basicity and adding C O 2 in the feed on the oxidative coupling of methane over K20 and SrO promoted LazO3/ZnO catalysts, 1997
- [12] Y. Cai, L. Chou, S. Li, B. Zhang, J. Zhao, Selective conversion of methane to C2 hydrocarbons using carbon dioxide over Mn-SrCO3 catalysts, Catal. Lett. 86 (4) (2003) 191–195, https://doi.org/10.1023/A:1022607800345.
- [13] Y. Wang, Y. Takahashi, Y. Ohtsuka, Effective catalysts for conversion of methane to ethane and ethylene using carbon dioxide, Chem. Lett. 27 (12) (1998) 1209–1210, https://doi.org/10.1246/cl.1998.1209.
- [14] Y. Wang, Y. Ohtsuka, Mn-based binary oxides as catalysts for the conversion of methane to C2 hydrocarbons with carbon dioxide as oxidant, Appl. Catal. A: Gen. 219 (1) (2001) 183–193, https://doi.org/10.1016/S0926-860X(01)00684-6.
- [15] Y. He, B. Yang, G. Cheng, On the oxidative coupling of methane with carbon dioxide over CeO2/ZnO nanocatalysts, Catal. Today 98 (4) (2004) 595–600, https://doi.org/10.1016/j.cattod.2004.09.014.
- [16] Istadi, N.A.S. Amin, Synergistic effect of catalyst basicity and reducibility on performance of ternary CeO2-based catalyst for CO₂ OCM to C2 hydrocarbons, J. Mol. Catal. A: Chem. 259 (1) (2006) 61–66, https://doi.org/10.1016/j. molcata.2006.06.003.
- [17] Y. Zhang, et al., CO₂ oxidative coupling of methane using an earth-abundant Ca0-based catalyst, Sci. Rep. 9 (1) (2019) 15454, https://doi.org/10.1038/s41598-019-51817-2.
- [18] B. Litawa, P. Michorczyk, J. Ogonowski, Influence of Co₂ on the catalytic performance Of La ₂ O ₃ /CeO₂ and CaO/CeO₂ catalysts in the oxidative coupling of methane, Pol. J. Chem. Technol. 15 (1) (2013) 22–26, https://doi.org/10.2478/ pjct-2013-0005.
- [19] S.J. Korf, J.A. Roos, N.A. de Bruijn, van Ommen, J.R.H. Ross, Influence of CO2 on the Oxidative Coupling of Methane over a Lithium Promoted Magnesium Oxide Catalyst, p. 2.
- [20] B. Rollins, N. Grosjean, S. Poulston, The impact of the presence of various relevant gases during aging of MnNa2WO4/SiO2 catalyst on its performance for the oxidative coupling of methane, Appl. Catal. A: Gen. 598 (2020) 117606, https:// doi.org/10.1016/j.apcata.2020.117606.
- [21] T. Levan, M. Che, J.M. Tatibouet, M. Kermarec, Infrared study of the formation and stability of La2O2CO3 during the oxidative coupling of methane on La2O3, J. Catal. 142 (1) (1993) 18–26, https://doi.org/10.1006/jcat.1993.1185.

- [22] S. Lacombe, H. Zanthoff, C. Mirodatos, Oxidative coupling of methane over lanthana catalysts, J. Catal. 155 (1) (1995) 106–116, https://doi.org/10.1006/ icat.1995.1192.
- [23] R.P. Taylor, G.L. Schrader, Lanthanum catalysts for methane oxidative coupling: a comparison of the reactivity of phases, Ind. Eng. Chem. Res. 30 (5) (1991) 1016–1023, https://doi.org/10.1021/ie00053a025.
- [24] C. Guan, et al., How CO_2 poisons La2O3 in an OCM catalytic reaction: a study by in situ XRD-MS and DFT, J. Catal. 396 (2021) 202–214, https://doi.org/10.1016/j.jcat.2021.02.017.
- [25] C. Estruch Bosch, Exploring the synthesis and use of lanthanum-based catalysts for oxidative coupling of methane, Ghent Univ. (2019).
- [26] C. Karakaya, R.J. Kee, Progress in the direct catalytic conversion of methane to fuels and chemicals, Prog. Energy Combust. Sci. 55 (2016) 60–97, https://doi.org/ 10.1016/j.pecs.2016.04.003.
- [27] L.A. Vandewalle, R. Van de Vijver, K.M. Van Geem, G.B. Marin, The role of mass and heat transfer in the design of novel reactors for oxidative coupling of methane, Chem. Eng. Sci. 198 (2019) 268–289, https://doi.org/10.1016/j.ces.2018.09.022.
- [28] J. Shi, L. Yao, C. Hu, Effect of CO₂ on the structural variation of Na2WO4/Mn/SiO2 catalyst for oxidative coupling of methane to ethylene, J. Energy Chem. 24 (4) (2015) 394–400, https://doi.org/10.1016/j.jechem.2015.06.007.
- [29] C. Chu, Y. Zhao, S. Li, Y. Sun, CO₂ chemisorption and its effect on methane activation in La₂ O₃ -catalyzed oxidative coupling of methane, J. Phys. Chem. C 120 (5) (2016) 2737–2746, https://doi.org/10.1021/acs.jpcc.5b10457.
- [30] C. Karakaya, H. Zhu, C. Loebick, J.G. Weissman, R.J. Kee, A detailed reaction mechanism for oxidative coupling of methane over Mn/Na2WO4/SiO2 catalyst for non-isothermal conditions, Catal. Today 312 (2018) 10–22, https://doi.org/ 10.1016/j.cattod.2018.02.023.
- [31] S. Sourav, Y. Wang, D. Kiani, J. Baltrusaitis, R.R. Fushimi, I.E. Wachs, New mechanistic and reaction pathway insights for oxidative coupling of methane (OCM) over supported Na₂ WO₄/SiO₂ catalysts, Angew. Chem. Int Ed. 60 (39) (2021) 21502–21511, https://doi.org/10.1002/anie.202108201.
- [32] H. Wang, et al., A Homogeneous-heterogeneous kinetic study of oxidative coupling of methane (OCM) on La 2O3 /CeO 2 catalyst, ChemCatChem 14 (23) (2022), https://doi.org/10.1002/cctc.202200927.
- [33] V.R. Choudhary, S.A.R. Mulla, B.S. Uphade, Oxidative coupling of methane over SrO deposited on different commercial supports precoated with La₂O₃, Ind. Eng. Chem. Res. 37 (6) (1998) 2142–2147, https://doi.org/10.1021/ie9706018.
- [34] Y. Gambo, et al., CO₂-mediated oxidative dehydrogenation of light alkanes to olefins: advances and perspectives in catalyst design and process improvement, Appl. Catal. A: Gen. 623 (2021) 118273, https://doi.org/10.1016/j. apcata.2021.118273.
- [35] M.L. Balogun, S. Adamu, I.A. Bakare, M.S. Ba-Shammakh, M.M. Hossain, CO₂ assisted oxidative dehydrogenation of propane to propylene over fluidizable MoO3/La2O3-γAl2O3 catalysts, J. CO₂ Util. 42 (2020) 101329, https://doi.org/10.1016/j.jcou.2020.101329.
- [36] G.A. Martin, C. Mirodatos, Surface chemistry in the oxidative coupling of methane, Fuel Process. Technol. 42 (2–3) (1995) 179–215, https://doi.org/10.1016/0378-3820(94)00093-9.
- [37] S. Yoon, S. Lim, J.-W. Choi, D.J. Suh, K.H. Song, J.-M. Ha, Study on the unsteady state oxidative coupling of methane: effects of oxygen species from O₂, surface lattice oxygen, and CO₂ on the C₂₊ selectivity, RSC Adv. 10 (59) (2020) 35889–35897, https://doi.org/10.1039/D0RA06065H.
- $[38] Y. Su, Upper bound on the yield for oxidative coupling of methane, J. Catal. 218 (2) \\ (2003) 321-333, https://doi.org/10.1016/S0021-9517(03)00043-5.$
- [39] S. Parishan, et al., Investigation into consecutive reactions of ethane and ethene under the OCM reaction conditions over MnxOy-Na2WO4/SiO2 catalyst, Catal. Lett. 148 (6) (2018) 1659–1675, https://doi.org/10.1007/s10562-018-2384-6.
- [40] Y.-H. Hou, W.-C. Han, W.-S. Xia, H.-L. Wan, Structure sensitivity of La₂O₂CO₃ catalysts in the oxidative coupling of methane, ACS Catal. 5 (3) (2015) 1663–1674, https://doi.org/10.1021/cs501733r.
- [41] Y. Watanabe, S. Miyazaki, T. Maruyama, Y. Saito, Dissociation pressure of lanthanum dioxide carbonate, J. Mater. Sci. Lett. 5 (2) (1986) 135–136, https://doi.org/10.1007/BF01672023.
- [42] J.P.H. Li, et al., Understanding of binding energy calibration in XPS of lanthanum oxide by in situ treatment, Phys. Chem. Chem. Phys. 21 (40) (2019) 22351–22358, https://doi.org/10.1039/C9CP04187G.
- [43] C.V. Ramana, R.S. Vemuri, V.V. Kaichev, V.A. Kochubey, A.A. Saraev, V. V. Atuchin, X-ray photoelectron spectroscopy depth profiling of La₂O₃/Si thin films deposited by reactive magnetron sputtering, ACS Appl. Mater. Interfaces 3 (11) (2011) 4370–4373, https://doi.org/10.1021/am201021m.
- [44] M.F. Sunding, K. Hadidi, S. Diplas, O.M. Løvvik, T.E. Norby, A.E. Gunnæs, XPS characterisation of in situ treated lanthanum oxide and hydroxide using tailored charge referencing and peak fitting procedures, J. Electron Spectrosc. Relat. Phenom. 184 (7) (2011) 399–409, https://doi.org/10.1016/j.elspec.2011.04.002.
- [45] M.M. Natile, A. Galenda, A. Glisenti, From La2O3 To LaCoO3: XPS analysis, Surf. Sci. Spectra 15 (1) (2008) 1–13, https://doi.org/10.1116/11.20061006.
- [46] X. Zhou, E.I. Vovk, Y. Liu, C. Guan, Y. Yang, An in situ temperature-dependent study of La2O3 reactivation process, Front. Chem. 9 (2021) 694559, https://doi. org/10.3389/fchem.2021.694559.

- [47] X. Zhou, et al., Active oxygen center in oxidative coupling of methane on La2O3 catalyst, J. Energy Chem. 60 (2021) 649–659, https://doi.org/10.1016/j.iechom.2021.01.008
- [48] S. Wang, S. Li, D.A. Dixon, Mechanism of selective and complete oxidation in La ₂ O ₃ -catalyzed oxidative coupling of methane, Catal. Sci. Technol. 10 (8) (2020) 2602–2614, https://doi.org/10.1039/DOCY00141D.
- [49] M.S. Palmer, M. Neurock, M.M. Olken, Periodic density functional theory study of methane activation over La₂O₃: activity of O ², O , O ₂ ², oxygen point defect, and Sr ²⁺ -doped surface sites, J. Am. Chem. Soc. 124 (28) (2002) 8452–8461, https://doi.org/10.1021/ja0121235.